A Platinum Poly-yne Featuring N-heterocyclic Carbene Ligands: Synthesis, Properties and Organic Light-Emitting Diode Application

Ru He,[a,b] Raquel Domingues,[b,c] Silvano Valandro[b] and Kirk S. Schanze[b]*

E-mail: kirk.schanze@utsa.edu

[a]Department of Chemistry, University of Florida, Gainesville, Florida 32611, USA

[b]Department of Chemistry, The University of Texas at San Antonio, San Antonio, Texas 78249, USA

[c]Institute of Science and Technology, Federal University of São Paulo, R. Talim, 330, São José dos Campos, São Paulo 12231-280, Brazil

ABSTRACT

We report the synthesis, characterization, and organic light-emitting diodes (OLEDs) application of the first example of a platinum poly-yne (**NPtAP**) featuring N-heterocyclic carbene (NHC) ligands. **NPtAP** was synthesized via Cu(I) catalyzed AA/BB type polymerization reaction with M_n = 8400 g-mol^{-1} and Đ = 1.6. The bulky and strong σ-donating NHC ligands bearing chiral 2-ethylhexyl substituents help to limit the interchain interaction and destabilize the non-emissive metal-centered d-d state, resulting in enhancement of the photoluminescence quantum yield of the platinum poly-yne. The prototype solution-processed OLEDs employing **NPtAP** as the emitter were successfully fabricated and display yellow-green electroluminescence (EL).

Introduction

Platinum poly-ynes are a fascinating class of organometallic π-conjugated polymers featuring efficient intersystem crossing and long-lived excited triplet states.[1] The early reports by

Hagihara on the synthesis of Pt(II) poly-ynes attracted considerable attention,[2-3] and subsequent studies explored the photophysical properties and applications of platinum poly-ynes with *trans*-configuration, e.g., *trans*-[-Pt(L)$_2$(C≡C-Ar-C≡C)-]$_n$).[4-8] Owing to their efficient singlet → triplet intersystem crossing, which is enabled by the heavy atom effect induced by the platinum atom, platinum poly-ynes display room-temperature phosphorescence from $^3\pi,\pi^*$ states.[5-6,8-14] Most of the reported platinum poly-ynes to date contain alkyl-phosphine ligands (PR_3); these phosphine ligands not only facilitate the solubility of platinum poly-ynes but they also provide a suitable coordination environment for the square planar Pt(II) center.[6,10,15-18] Despite the observation of room temperature phosphorescence from *trans*-Pt poly-ynes, their photoluminescence quantum yields, especially in the solid-state, are typically low (< 0.01).[19] Thermal population of non-emissive metal-centered excited triplet state (^{3}MC or ^{3}d-d) from $^3\pi,\pi^*$ state and interchain "excimer like" interactions were considered as the primary reasons for the low phosphorescence efficiency.[19]

Previous studies on phosphorescent metal complexes have demonstrated that strong σ-donating ligands destabilize the non-emissive ^{3}MC state by raising the energy of metal dσ* orbitals, enabling efficient luminescence from the triplet state.[20-22] N-heterocyclic carbenes (NHCs) are stable heterocyclic moieties with a carbene carbon and at least one nitrogen atom in the ring.[23] As strong σ-donors, NHC ligands have been widely employed in phosphorescent cyclo-metalated iridium complexes, in some cases giving rise to high quantum efficiency deep blue-emitting complexes.[24-27] The strong ligand-field strength of NHC ligands can push the metal-centered ^{3}d-d state to a relatively high energy, so that the non-emissive ^{3}d-d state becomes less thermally accessible. The incorporation of NHCs into *trans*-Pt(II) acetylide complexes also significantly enhances their phosphorescence efficiency when compared to their *trans*-Pt(PR_3)$_2$(C≡C-Ar)$_2$

analogues.[28-32] Efficient phosphorescence from acetylide ligand centered $^3\pi,\pi^*$ states with relatively high energy (2.8 eV) is observed, with quantum efficiencies greater than 0.50.[31,33] Good thermal and photochemical stability combined with efficient phosphorescence make *trans*-NHC Pt(II) acetylide complexes promising materials for optoelectronic applications.[31]

The current study is the first to explore the properties and organic light emitting diodes (OLEDs) application of a Pt(II) poly-yne in which the metal centers feature N-heterocyclic carbene ligands. The study is focused on the Pt(II) poly-yne polymer **NPtAP** (Chart 1) that contains two benzimidazole carbene ligands and a backbone based on the *trans*-$[(NHC)_2Pt\text{-}C{\equiv}C\text{-}Ar\text{-}C{\equiv}C\text{-}]_n$ architecture, where Ar is a bis-alkyl substituted phenylene unit. Solubility of the polymer was ensured by inclusion of two chiral 2-ethylhexyl chains on each NHC ligand and bis-dodecyl chains on the phenylene units. The strong ligand field strength NHC ligands are believed to push the ^{3}d-d state of Pt(II) centers to a relatively high energy, and this effect combined with the steric hindrance offered by the bulky NHC ligands limits the interchain interaction and Pt-Pt interactions in the solid-state. These effects give rise to relatively efficient phosphorescence in solution and in a solid poly(methyl methacrylate) (PMMA) host matrix.. The photophysical properties of the polymer were fully characterized in both THF solution and in PMMA host matrix by using UV-visible absorption, steady-state emission spectroscopy, time-resolved emission spectroscopy and transient absorption (TA) spectroscopy. Prototype solution-processed OLEDs with **NPtAP** as the emitter display yellow-green electroluminescence (EL). This work provides a novel alternative to small-molecule phosphor-based OLEDs that are fabricated by vacuum thermal deposition.

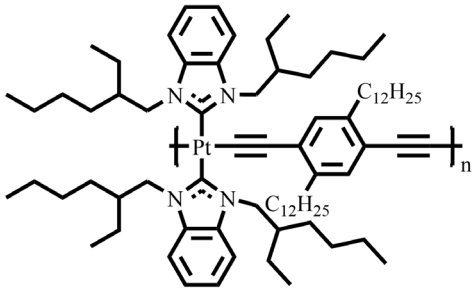

Chart 1. Structure of **NPtAP**.

Results and Discussion

Synthesis and Structural Characterization. The structure of the *trans*-NHC Pt(II) acetylide polymer **NPtAP** is shown in **Chart 1**. The polymer features a platinum-acetylide backbone with N-heterocyclic carbene ligands coordinated to the Pt(II) center. Polymerization was effected via a Cu(I) catalyzed AA/BB Hagihara polymerization reaction between **BiPtCl$_2$-EH** and 1,4-didodecyl-2,5-diethynylbenzene, eq. 1.

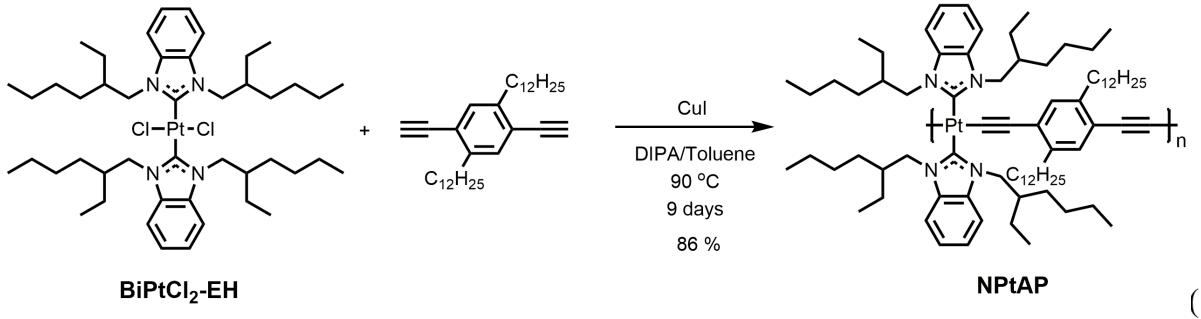

BiPtCl$_2$-EH **NPtAP** (1)

Details concerning the synthesis and characterization of the monomers are provided in the supplemental information section. Note that racemic 2-ethylhexyl iodide was used to prepare the 2-ethylhexyl substituted NHC ligands; thus, the monomer complex **BiPtCl$_2$-EH** is a mixture of four diastereomers based on the configurations of the four chiral carbons (RR/RR, RS/RR, RS/RS, SS/RR). The monomer complex **BiPtCl$_2$-EH** was prepared through a one-pot/two-steps method involving the *in-situ* formation of an Ag(I)-NHC intermediate and subsequent transmetalation of the Ag(I)-NHC intermediate with K_2PtCl_4. The *trans* geometry of **BiPtCl$_2$-EH** is inferred from

previous studies of related $(NHC)_2PtCl_2$ complexes that were prepared by the same route and their structure confirmed by single crystal X-ray diffraction analysis.[30,33] The sample of **NPtAP** derived from the 9 day polymerization reaction was first purified by size-exclusion chromatography to remove low molecular weight impurities.

The structure of polymer **NPtAP** was confirmed by ^1H NMR spectroscopy (Figure 1). In particular, at 7.2 -7.5 ppm, two characteristic peaks due to the aromatic protons of the NHC ligands are observed, while the protons on the phenylene rings are upfield at ~ 6.5 ppm. The N-**CH_2**-protons appear as a peak at ~ 4.7 ppm which is broad and complex due to the adjacent chiral centers. The methylene protons of phenyl-**CH_2**-$C_{11}H_{23}$ and the N-CH_2-**CH**$(C_2H_5)(C_4H_9)$ chiral methine proton appear as broad peaks at 2.31 and 2.16 ppm, respectively. A series of broad and strong peaks between 0.5 ppm and 1.7 ppm are due to all remaining protons on the six alkyl chains in the repeat unit. The integrations of all the peaks correspond with the structure of **NPtAP** (Figure S13 in the Supporting Information). The variable temperature NMR spectrum of polymer **NPtAP** at over the range 25 – 75 ^oC in C_6D_6 is shown in the Supporting Information (Fig. S14).

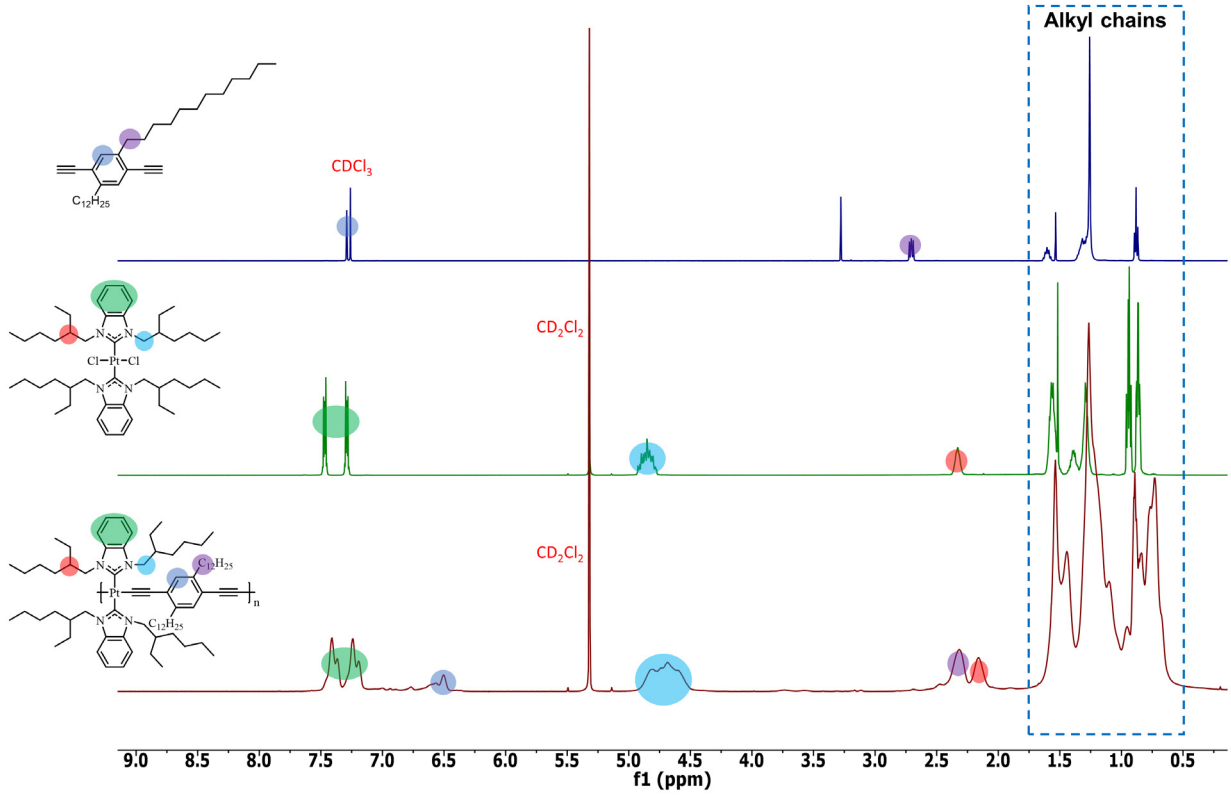

Figure 1. ^{1}H NMR spectra of monomers and **NPtAP**.

The molecular weight of **NPtAP** was determined by gel permeation chromatography (GPC) using polystyrene standards in THF giving rise to M_n = 8400 and Đ = 1.6 (Figure S15 in the Supporting Information). Taking into consideration the molecular mass of the repeat units (1341 g·mol^{-1}), the GPC derived M_n value leads to a number average degree of polymerization, DP_n = 6. It is well-established that GPC analysis of semi-rigid rod polymers such as poly(phenylene ethynylene), poly(phenylene–butadiynylene) and Pt-poly-ynes gives rise to over-estimated molecular weight (M_n) values when referenced to polystyrene.[3,34-35] However, an opposing trend is expected due to the relatively large molar mass of the $(NHC)_2Pt$ repeat units (1341 g·mol^{-1}). Taken together, we posit that the number average DP of the is likely a relatively good estimate of the average chain length in the **NPtAP** polymer.

Thermal analysis of **NPtAP** reveals that in inert atmosphere the polymer is stable up to ~280 °C, above which mass loss is observed (Fig. S16). The thermal stability of the polymer is comparable to that of molecular complexes that feature *trans*-$(NHC)_2Pt(-CC)_2$ units.[31]

Photophysical Properties. The absorption and emission spectra of **NPtAP** in THF solution are shown in Figure 2 and the corresponding photophysical properties are summarized in Table 1. The absorption of **NPtAP** displays a single featureless band arising from the long-axis polarized π,π* transition (Figure 2).[11-12] The absorption maximum is 371 nm with a molar extinction coefficient of 38,800 M^{-1} cm^{-1}, which is similar to the absorption of previously reported platinum poly-ynes.[19,36] The photoluminescence of **NPtAP** in degassed THF and doped at 0.2 wt% in a PMMA host polymer is also shown in Figure 2. In solution and in the PMMA matrix, the photoluminescence spectrum of **NPtAP** is dominated by intense phosphorescence from the ligand-centered ^{3}π,π* state.[4,19,37] No obvious fluorescence is observed signaling that intersystem crossing is efficient (*vide infra*). In THF, the phosphorescence of **NPtAP** features a strong band at 518 nm and two shoulder peaks at 559 nm and 583 nm, while in PMMA, only an emission maximum (518 nm) and a vibronic shoulder (559 nm) are observed. The third relatively weak peak at ~ 583 nm in THF is possibly due to **NPtAP** aggregates.[19] When doped into the PMMA matrix, the polymer chains are well-dispersed and the aggregate emission is not seen. Finally, the emission from a neat polymer film prepared by drop-casting was examined and the spectrum is similar to that observed in solution (see Fig. S17).

In degassed THF solution, the photoluminescence quantum yield of **NPtAP** is 0.049, which is 10-fold higher than previously reported platinum acetylide polymer with PBu_3 ligands (Φ_p = 0.0045).[19] The enhancement of the quantum yield can be attributed to the destabilization of the ^{3}d-d state combined with a restriction of interchain interactions induced by bulky σ-donating NHC

ligands. In PMMA, the quantum yield increases to 0.064, owing to the further reduction of non-radiative rotational/vibrational relaxation in the rigid environment. The phosphorescence yield of **NPtAP** as a neat polymer film is significantly lower than in solution (Table 1), suggesting that interchain interactions lead to triplet quenching. **NPtAP** shows a phosphorescence lifetime of 55 μs in THF and the emission lifetime increases to 74 μs in PMMA. Based on the quantum yield and lifetime values in THF, the radiative and non-radiative decay rates are 8.9 x 10^2 and 1.7 x 10^4 s^{-1}, respectively.

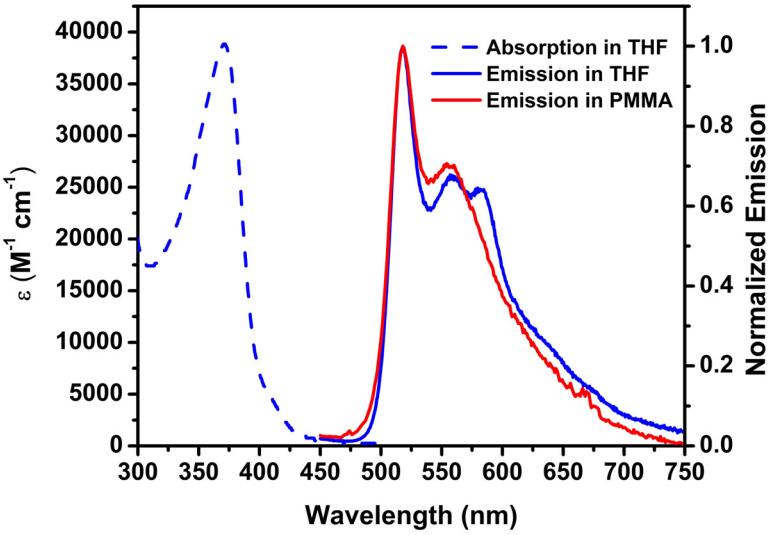

Figure 2. Absorption and emission of **NPtAP** in THF solution (c = 4.22 μmol/L) and doped in a PMMA matrix (0.2 wt% polymer).

Table 1. Photophysical Properties of **NPtAP**.

NPtAP	**Absorption**		**Photoluminescence**				
	λ_{max}	ε (M^{-1} cm^{-1})	λ_{max}	Φ_{PL}	τ_{PL}	k_r / s^{-1} [a]	k_{nr} / s^{-1} [a]
THF	371 nm	38839 (371 nm)	518 nm	0.049	55 μs	8.9 x 10^2	1.7 x 10^4
Neat Film	-	-	518 nm	0.0031	-	-	-
PMMA	-	-	518 nm	0.064	74 μs	8.6 x 10^2	1.3 x 10^4

[a] $\Phi_{PL} = k_r/(k_r + k_{nr})$ and $\tau_{PL} = 1/(k_r + k_{nr})$, therefore $k_r = \Phi_{PL}/\tau_{PL}$, $k_{nr} = 1/\tau_{PL} - k_r$.

Overall, the photophysical properties of **NPtAP** are similar to those of structurally-similar molecular complexes that have been previously studied. For example, the phosphorescence of *trans*-$(NHC)_2Pt(-C\equiv C-Ph-C\equiv C-Ph)_2$, where Ph = phenylene, features λ_{max} = 531 nm, Φ_p = 0.54 and τ = 575 μs.[38] The molecular complex exhibits $k_r = 9.4 \times 10^2\ s^{-1}$ and $k_{nr} = 8.0 \times 10^2\ s^{-1}$. Comparison here shows that polymer **NPtAP** has a comparable radiative decay rate, but a substantially higher non-radiative decay rate compared to the molecular chromophore. This effect may be due to quenching of the triplet exciton state by polymer end groups, aggregation or other exciton trap states present in the polymer that lead to enhanced non-radiative decay.

Nanosecond and Femtosecond Transient Absorption. Figure 3a shows the nanosecond transient absorption (ns-TA) spectra of **NPtAP** obtained in THF solution following 355 nm excitation. The spectrum is characterized by a strong bleach of the ground-state absorption in the near-UV and a broad transient absorption band in the visible region. The transient absorption band can be assigned to $T_1 \rightarrow T_n$ transitions, which have π- π* character.[19] The triplet-triplet absorption of **NPtAP** is very similar to that for the related polymers and oligomers of the type *trans*-[-Pt$(PBu_3)_2$-CC-Ar-CC-]$_n$.[39] This similarity is not surprising given that the triplet exciton is largely of π,π* character localized on the CC-Ar-CC units. Thus, the NHC ligands have little effect on the photophysics of the triplet exciton state. The triplet absorption decays with a lifetime of 68 μs and is consistent with the lifetime with that determined by time-resolved photoluminescence.

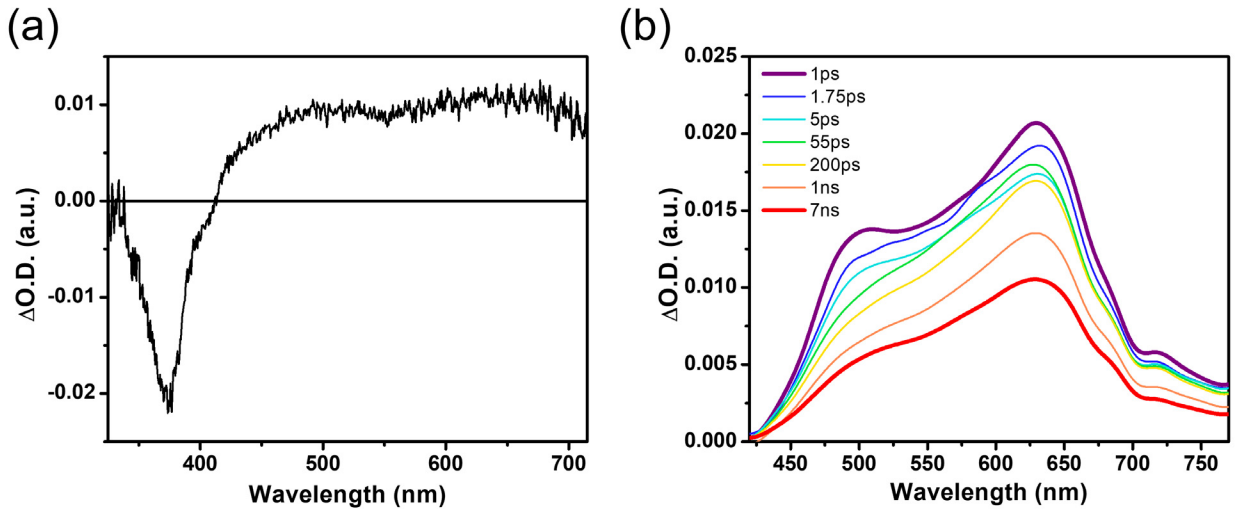

Figure 3. (a) ns-Transient absorption (TA) and (b) fs-TA spectra of **NPtAP** in THF. The ns-TA spectrum (at 25 ns delay) was obtained in deoxygenated THF solution following 355 nm excitation. The fs-TA spectrum was obtained in THF solution following 340 nm excitation.

The ultrafast transient absorption spectrum was obtained in THF solution under 340 nm laser excitation (Figure 3b). At early time delays, the TA spectrum of **NPtAP** is dominated by a transient absorption band with a maximum at 630 nm and a shoulder band around 500 nm. These bands are correlated since they decay together with the same time constants (Figure S18). After 7 ns, the transient absorption remains as a band at 630 nm with a weaker band at 500 nm; this spectrum resembles the triplet-triplet transient absorption seen in the ns-TA spectrum (Figure 3a). It is likely that the initial spectrum (~ 1 ps) is due to $^{1}\pi$-π^* exciton in **NPtAP**.[40] The following spectral changes that occur from 1 ps to 7 ns time delay are due to the singlet-triplet intersystem crossing (ISC) and subsequent vibrational relaxation in the triplet excited state. The ISC and the vibrational relaxation of the triplet state of **NPtAP** in THF were determined to be 0.8 ps (k_{ISC} = 1.25 x 10^{-12} s^{-1}) and 1050 ps, respectively. A similar ultrafast intersystem crossing rate was observed by Vardeny and co-workers for a Pt(II) poly-yne with similar structure, except the NHC ligands are replaced by tributyl phosphine ($P(nBu)_3$) ligands.[40]

Organic Light-Emitting Diodes. There is continuing interest in the development of phosphorescent materials for application light emitting devices.[41-45] A limited number of studies have examined Pt(II) poly-ynes for electrophosphorescent applications.[46-48] This is in part due to their relatively low phosphorescence efficiency. Given that the NHC based Pt(II) poly-yne **NPtAP** displays a moderately efficient green phosphorescence in solution and in PMMA matrix, we attempted to incorporate the polymer into solution processed organic light emitting diode (OLED) structures. Initial experiments focused on using neat films of **NPtAP** as the active layer; however, with repeated efforts these devices failed. Thus, we turned to a device structure consisting of an active layer containing **NPtAP** blended with a host matrix consisting of poly(vinyl carbazole) (PVK, hole transport) and 2-(4-biphenyl)-5-(4-tert-butylphenyl)-1,3,4-oxadiazole (PBD) as electron transporter.[48] The complete device architecture used is shown in Figure 4a: ITO/PEDOT:PSS (30 nm)/ PVK:PBD (27 wt%): **NPtAP** (5 or 10 wt%) (60 nm)/ LiF (1 nm)/Al (100 nm). The chemical structures of all organic materials used in OLED fabrication are shown in Figure S19. ITO and Al were employed as the anode and cathode, respectively. PEDOT:PSS was used as the hole injection layer, and LiF was used to lower the barrier for electron injection.

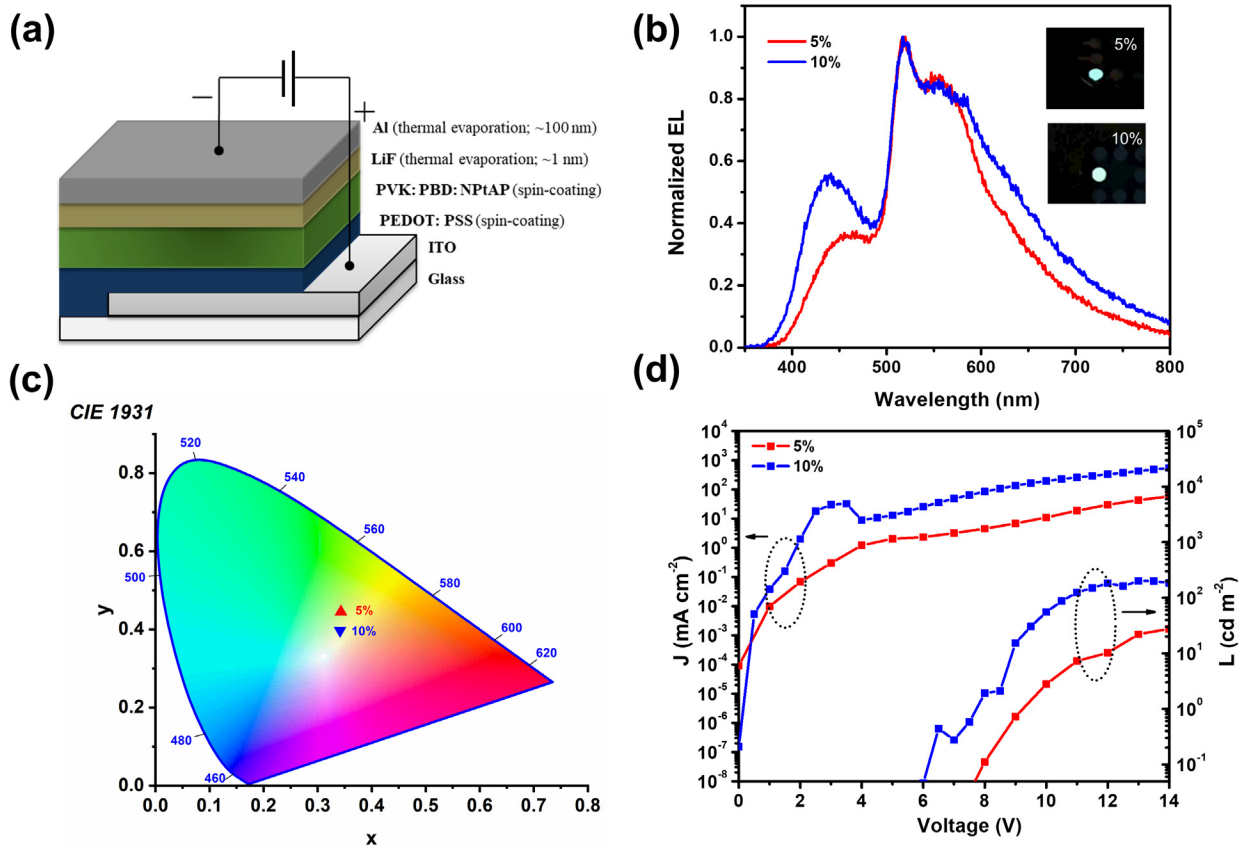

Figure 4. (a) Device architecture: ITO/ PEDOT:PSS /PVK: PBD: **NPtAP** (5 or 10 wt%)/ LiF/ Al; (b) EL Spectra (9 V). Inset: photo of OLEDs; (c) CIE coordinates for the OLEDs; (d) *J*-*V*-*L* characteristics (*J*= current density, *L*= luminance).

The structure, electroluminescence (EL) spectra, CIE chromaticity diagram, and *J*-*V*-*L* characteristics of the **NPtAP** devices are shown in Figure 4 and Table 2. EL spectra at different drive voltages are shown in the SI (Figs. S21 and S22). The device with 5 wt% of **NPtAP** in the emissive layer shows an EL emission with a maximum at 518 nm and a shoulder at 559 nm, exhibiting a similar feature to the solid-state phosphorescence spectrum of **NPtAP** in PMMA. In contrast, the OLED with 10 wt% of **NPtAP** displays EL with a maximum at 518 nm and two shoulders (559 nm and 583 nm), which is similar to the PL of **NPtAP** in THF, where aggregation is believed to contribute to the phosphorescence. The additional shoulder peak at 583 nm is

possibly due to aggregation of **NPtAP** in the PVK:PBD matrix when the amount of **NPtAP** in the blend is higher. Unfortunately, in both device structures a broad high-energy emission is observed at around 440 nm. A similar weak emission is observed in the photoluminescence spectrum of the neat **NPtAP** film (Fig. S17). This short wavelength electroluminescence band is possibly due to fluorescence from **NPtAP**, or it could be attributed to the emission from the PVK host or a PBD:PVK exciplex.[49-51] The high-energy band around 440 nm becomes more intense relative to the **NPtAP** electroluminescence for the device with 10 wt% of **NPtAP**.

Table 2. Device Characteristics of OLEDs

NPtAP (wt %)	J (mA/cm^2)[a]	EQE% $_{max}$ [b]	CIE 1931 [c] (x,y)	$\lambda_{max/nm}$	L_{max} (Cd/m^2)	CE$_{max}$ (Cd/A)
5%	42	0.019	0.34, 0.45	519	31	0.006
10%	326	0.022	0.34, 0.40	519	188	0.04

[a]Values of current density were obtained at the maximum EQE; [b]OLED external quantum efficiency at maximum; [c]CIE 1931 color coordinates.

The OLEDs performance are summarized in Table 2. The Commission Internationale d'Eclairage (CIE) coordinates of **NPtAP** based OLEDs are shown in Figures 4c. The OLEDs containing 10 wt% **NPtAP** shows a white EL with CIE coordinates of (0.34, 0.40). For the device with 5 wt% of **NPtAP**, the high-energy emission band is suppressed, and the EL spectrum is more closely matched the PL of **NPtAP**. The device exhibits a yellow-green EL with CIE coordinates of (0.34, 0.45). The maximum external quantum efficiencies (EQEs) of these OLEDs are relatively low, 0.019% for the device with 5 wt% of **NPtAP** and 0.022% for the device with 10 wt% of **NPtAP** (Figure S20). The low EQE of the **NPtAP** devices mirrors the relatively low PL quantum efficiency of the polymer in the neat solid films, suggesting that the polymer may not be well dispersed into the PVK:PBD host.

Although the performance of these prototype devices is unimpressive, this is, to the best of our knowledge, the first example of employing platinum(II) acetylide polymer featuring NHC ligands as the emitter in a phosphorescent OLED. Further device engineering and host material

selection should be able to achieve spectrally pure EL from **NPtAP** and improve the performance of the devices.

General Discussion

This paper reports the synthesis and characterization of a platinum poly-yne that contains NHC ligands at the Pt(II) center. A number of recent reports have provided strong indication that the optical properties of the platinum acetylides are enhanced by the NHC ligands. Specifically, in several recent reports, deep blue, sky blue and green phosphors based on Pt(II) NHC acetylides have been reported that exhibit high phosphorescence quantum efficiency.[28-32] The small molecule complexes have also been reported to perform well in vapor deposited OLEDs and in some cases devices operate with EQE > 10%.[33] These prior reports were drivers to this work, which had the goal of constructing a platinum poly-yne that exhibits high phosphorescence yield and potentially good performance in a solution processed OLED.

Before the successful polymerization reaction that is reported here was achieved, a number of polymerizations were carried out that failed to produce a polymeric product. In particular, reaction of **BiPtCl$_2$-EH** with 1,4-diethynyl benzene did not afford a polymeric product, due to precipitation of the intermediates (oligomers) during polymerization. Polymerization was also attempted using an analog of **BiPtCl$_2$-EH** in which the N-ethylhexyl chains are replaced by -$(CH_2CH_2$-O-$)_3$-CH_3 groups, but the resulting material was insoluble. Moreover, the successful reaction (eq. 1) is slow, requiring 9 days to reach M_n = 8400 g-mol^{-1}. By comparison, typical Hagihara polymerizations are carried out in 24 hours.[2-3] The slow reaction of **BiPtCl$_2$-EH** with the substituted 1,4-diethynylbenzene co-monomer is likely due to unfavorable steric interactions between the ethylhexyl substituted NHC and phenylene units which hinder approach between the monomers

necessary for the coupling reaction to occur. Unfortunately, these bulky alkyl groups are necessary to ensure solubility of the polymer.

The photophysical properties of **NPtAP** are similar to those of structurally-related platinum poly-ynes that have been previously reported based on phosphine supporting ligands (e.g., *trans*-[-Pt(PBu_3)$_2$(C≡C-Ph-C≡C)-]$_n$ where Ph = 1,4-phenylene).[4,9,19] The emission arises from a $^3\pi,\pi*$ state that is mainly localized on the 1,4-diethynylbenzene unit.[40,52] As noted above, there is some evidence that the emission of **NPtAP** in THF solution could be broadened due to the presence of inter- or intrachain aggregates. A previous study of phosphine substituted analog polymer -[-Pt(PBu_3)$_2$(C≡C-Ph-C≡C)-]$_n$ revealed evidence for a longer wavelength emission that arises from an aggregated state of the polymer.[19] It is surprising that given the steric hindrance in the **NPtAP** that aggregation can occur, but nevertheless it remains a possibility. Interestingly, the emission lifetime of **NPtAP** is considerably longer compared to the phosphine analog (55 μs vs. ~1 μs).[19] The significant difference is likely due to a lower non-radiative decay rate in **NPtAP**.

The prototype OLED work demonstrates the potential for the organometallic polymers featuring NHC ligands in optoelectronic application. Nevertheless, the overall performance of the **NPtAP** devices is low, with EQE < 0.1% and maximum luminance ~200 Cd-m^{-2}. The performance of the material parallels that of a Pt(II) acetylide featuring bithiazole repeating units and a white-emitting Pt poly-yne,[47,53] but it is considerably less than an Pt(II) acetylide analog that featured carbazole repeats.[48] One reason for the low EL performance is due to inefficient electron and/or hole transfer from the host to the polymer. While these are shortcomings in the current prototype study, it is likely that further device engineering, including the use of optimized hole and electron injection layers can lead to substantial improvement in performance.

Conclusion

A novel trans-NHC platinum(II) acetylide polymer **NPtAP** was successfully synthesized and fully characterized. The incorporation of NHC ligands leads to a substantial enhancement in phosphorescence quantum yield compared to the platinum(II) acetylide polymer featuring phosphine ligands. This can be attributed to the strong σ-donating nature of the bulky NHC ligands, which destabilize the metal-centered d-d state and limit the interchain interaction. Prototype OLEDs employing **NPtAP** as the emitter were successfully fabricated and display yellow-green EL. Further device engineering may help to improve the performance of the OLEDs.

Experimental Section

Materials. All chemicals were purchased from either Sigma-Aldrich or Fisher Scientific unless otherwise noted and used without further treatment. Potassium tetrachloroplatinate(II) and *trans*-dichlorobis(triphenylphosphine)palladium(II) were purchased from Strem Chemicals, Inc.. Solvents were of reagent grade unless otherwise noted. Dry solvents (HPLC grade) were obtained from an MBraun MB-SPS-800 solvent purification system. Bio-Beads^{TM} S-X1 (200-400 mesh) was purchased from Bio-Rad. Details concerning the synthesis and characterization of monomers and **NPtAP** are provided in the supporting information section.

Purification. Reactions were monitored by silica gel TLC plates, visualized with ultraviolet light. Column chromatography (silica) was performed using CombiFlash Rf+ (Teledyne-Isco) automated flash chromatography system.

Characterization. ^{1}H (500 MHz) and ^{13}C (125 MHz) NMR spectra were recorded on a Bruker 500 MHz Avance III HD spectrometer. The chemical shifts were reported in ppm relative to protonated solvent peaks in ^{1}H and ^{13}C NMR spectra. High-resolution mass spectrometry (HR-MS) was performed by Mass Spectrometry Services at the University of Texas at San Antonio. HR-MS data was collected on a MaXis Plus quadrupole-time-of-flight mass spectrometer

equipped with an electrospray ionization source (Bruker Daltonics) and operated in the positive ionization mode. Gel permeation chromatography (GPC) analysis was carried out on a EcoSEC GPC system comprised of two independently operating pumps, TSKgel MultiporeHxl-M column and RI and UV detectors, with THF as eluent at 1 mL/min flow rate. The system was calibrated against linear polystyrene standards in THF.

Photophysical Studies. The UV-visible absorption spectrum was obtained on a Shimadzu UV-1800 dual-beam spectrophotometer. Steady-state photoluminescence measurements were performed on an Edinburgh FLS1000 spectrophotometer. Phosphorescence quantum yield of the **NPtAP** polymer glass was obtained with respect to pure PMMA glass in an Edinburgh N-M01 integrating sphere accessory to the FLS1000. Phosphorescence quantum yield of the solution was measured in nitrogen bubble-degassed THF with respect to $Ru(bpy)_3Cl_2$ (Φ =0.038) in aerated deionized water. Phosphorescence lifetime and nanosecond transient absorption measurements were obtained on Edinburgh LP980 transient absorption spectrometer using a Continuum Surelite II series Nd:YAG laser (3rd harmonic λ = 355 nm, 5 mJ per pulse) as the excitation source. Ultrafast transient absorption data were collected using pump-probe techniques with a 120 fs, 1 kHz Ti:sapphire Coherent Astrella laser as the excitation source. The pump beam was generated using a portion of the 800 nm amplifier beam by being directed into a Coherent OPerA Solo ultrafast optical parametric amplifier, which was tuned to generate a beam of light of 340 nm. The pump beam was then directed into an Ultrafast Systems Helios Fire automated femtosecond transient absorption spectrometer where the beam passed through a mechanical chopper, depolarizer, and neutral density filter to tune the beam to 0.1 mW (100 nJ/pulse) of power before hitting the stirred sample (~0.4 O.D.). Another portion of the 800 nm beam was directed into the Helios Fire directed into an automated 8 ns delay stage, afterward, the beam was focused into a

sapphire plate to generate a visible probe ranging from 430 to 770 nm. The visible signal was detected using a fiber-coupled spectrometer with a 1024 pixel CMOS sensor. The time delay between the pump and probe is controlled using the computer software-controlled delay stage.

OLED Fabrication and Testing. The devices were fabricated on glass substrates commercially precoated with a layer of indium tin oxide (ITO) with a sheet resistance of ~15 Ω/sq. The substrates were cleaned with dodecyl sulfate solution, Millipore water, acetone, and isopropanol in an ultrasonic bath, for 15 min each, and then exposed to the oxygen plasma for 20 min. OLEDs were fabricated in a glove box (H_2O, O_2 < 1 ppm) with the configuration of ITO/ PEDOT: PSS (30 nm)/ PVK: PDB (27 wt%): **NPtAP** (5 or 10 wt%) (60 nm)/ LiF (1 nm)/ Al (100 nm). A 30 nm layer of PEDOT:PSS was deposited by spin-coating (5000 rpm, 40 s) onto the ITO-glass substrate and annealed at 130 °C for 30 min on a hotplate. Then, the emissive layer (60 nm) was spin-coated (2000 rpm, 60 s) from a mixed chlorobenzene solution of PVK, PBD and **NPtAP**. Finally, 1 nm of LiF and 100 nm of aluminum were deposited via vacuum thermal evaporation under the pressure of ~10^{-6} mbar in an MBraun-Evaporator glovebox. The OLEDs were sealed using encapsulation epoxy, allowing the manipulation and characterization under ambient conditions.

The electroluminescence spectra of the OLEDs were obtained using an Ocean Optics spectrometer (USB 2000) and a Keithley 2450 power source. Current density-Voltage-Luminance (*J-V-L*) characteristics and radiant power of the devices were measured using a Keithley 2450 power source and a photodiode connected to an Optometer (UDT, model S471). All data were collected using a homemade LabView® interface. The external quantum efficiencies (EQEs) were then calculated from luminance and device spectra.

Associated Content

Supporting Information

The Supporting Information is available free of charge on the ACS Publication website at DOI: Experimental details, NMR spectra, GPC data, TGA analysis, photophysical properties measurements, photoluminescence lifetime data and OLED data.

AUTHOR INFORMATION

Corresponding Author

Kirk S. Schanze: Department of Chemistry, The University of Texas at San Antonio, San Antonio, Texas 78249, USA; ORCID ID: http://orcid.org/0000-0003-3342-4080, Email: kirk.schanze@utsa.edu.

Authors

Ru He: Department of Chemistry, University of Florida, Gainesville, Florida 32611, USA; Department of Chemistry, The University of Texas at San Antonio, San Antonio, Texas 78249, USA.

Raquel Domingues: Institute of Science and Technology, Federal University of São Paulo, R. Talim, 330, São José dos Campos, São Paulo 12231-280, Brazil; Department of Chemistry, The University of Texas at San Antonio, San Antonio, Texas 78249, USA.

Silvano Valandro: Department of Chemistry, The University of Texas at San Antonio, San Antonio, Texas 78249, USA; ORCID ID: http://orcid.org/0000-0002-4652-768X

Author Contributions

† R.H. and R.D. contributed equally to this work.

Notes

The authors declare no competing financial interest.

Acknowledgements

This work was supported by the National Science Foundation (Grant No. CHE-1904288). R.D. acknowledges support from the São Paulo Research Foundation (FAPESP. Grant #2019/06882-1). Partial support for R.D.'s effort on this project was provided through the Welch Chair at the University of Texas at San Antonio (Award AX-0045-20110629).

References

1. Haque, A.; Al-Balushi, R. A.; Al-Busaidi, I. J.; Khan, M. S.; Raithby, P. R., Rise of Conjugated Poly-ynes and Poly (Metalla-ynes): From Design through Synthesis to Structure–Property Relationships and Applications. *Chem. Rev.* **2018,** *118*, 8474-8597.
2. Sonogashira, K.; Takahashi, S.; Hagihara, N., A New Extended Chain Polymer, Poly[Trans-Bis(Tri-N-Butylphosphine)Platinum 1,4-Butadiynediyl]. *Macromolecules* **1977,** *10*, 879-880.
3. Takahashi, S.; Kariya, M.; Yatake, T.; Sonogashira, K.; Hagihara, N., Studies of Poly-yne Polymers Containing Transition Metals in the Main Chain. 2. Synthesis of Poly[trans-Bis(tri-N-Butylphosphine)Platinum 1,4-Butadiynediyl] and Evidence of a Rodlike Structure. *Macromolecules* **1978,** *11*, 1063-1066.
4. Wittmann, H.; Friend, R.; Khan, M.; Lewis, J., Optical Spectroscopy of Platinum and Palladium Containing Poly-ynes. *J. Chem. Phys.* **1994,** *101*, 2693-2698.
5. Chawdhury, N.; Köhler, A.; Friend, R. H.; Younus, M.; Long, N. J.; Raithby, P. R.; Lewis, J., Synthesis and Electronic Structure of Platinum-Containing Poly-ynes with Aromatic and Heteroaromatic Rings. *Macromolecules* **1998,** *31*, 722-727.
6. Khan, M. S.; Al-Mandhary, M. R.; Al-Suti, M. K.; Feeder, N.; Nahar, S.; Köhler, A.; Friend, R. H.; Wilson, P. J.; Raithby, P. R., Synthesis, Characterisation and Electronic Properties of a Series of Platinum (II) Poly-ynes Containing Novel Thienyl-Pyridine Linker Groups. *J. Chem. Soc. Dalton* **2002**, 2441-2448.

7. Wu, W.; Zhang, J.; Yang, H.; Jin, B.; Hu, Y.; Hua, J.; Jing, C.; Long, Y.; Tian, H., Narrowing Band Gap of Platinum Acetylide Dye-Sensitized Solar Cell Sensitizers with Thiophene π-Bridges. *J. Mater. Chem.* **2012,** *22*, 5382-5389.
8. Wong, W.-Y.; Ho, C.-L., Di-, Oligo- and Polymetallaynes: Syntheses, Photophysics, Structures and Applications. *Coord. Chem. Rev.* **2006,** *250*, 2627-2690.
9. Beljonne, D.; Wittmann, H. F.; Köhler, A.; Graham, S.; Younus, M.; Lewis, J.; Raithby, P. R.; Khan, M. S.; Friend, R. H.; Brédas, J. L., Spatial Extent of the Singlet and Triplet Excitons in Transition Metal-Containing Poly-ynes. *J. Chem. Phys.* **1996,** *105*, 3868-3877.
10. Chawdhury, N.; Köhler, A.; Friend, R. H.; Wong, W.-Y.; Lewis, J.; Younus, M.; Raithby, P. R.; Corcoran, T. C.; Al-Mandhary, M. R.; Khan, M. S., Evolution of Lowest Singlet and Triplet Excited States with Number of Thienyl Rings in Platinum Poly-ynes. *J. Chem. Phys.* **1999,** *110*, 4963-4970.
11. Wilson, J. S.; Chawdhury, N.; Al-Mandhary, M. R.; Younus, M.; Khan, M. S.; Raithby, P. R.; Köhler, A.; Friend, R. H., The Energy Gap Law for Triplet States in Pt-Containing Conjugated Polymers and Monomers. *J. Am. Chem. Soc.* **2001,** *123*, 9412-9417.
12. Liu, Y.; Jiang, S.; Glusac, K.; Powell, D. H.; Anderson, D. F.; Schanze, K. S., Photophysics of Monodisperse Platinum-Acetylide Oligomers: Delocalization in the Singlet and Triplet Excited States. *J. Am. Chem. Soc.* **2002,** *124*, 12412-12413.
13. Ho, C.-L.; Yu, Z.-Q.; Wong, W.-Y., Multifunctional Polymetallaynes: Properties, Functions and Applications. *Chem. Soc. Rev.* **2016,** *45*, 5264-5295.
14. Xu, L.; Ho, C.-L.; Liu, L.; Wong, W.-Y., Molecular/Polymeric Metallaynes and Related Molecules: Solar Cell Materials and Devices. *Coord. Chem. Rev.* **2018,** *373*, 233-257.

15. Cooper, T. M.; Krein, D. M.; Burke, A. R.; McLean, D. G.; Rogers, J. E.; Slagle, J. E.; Fleitz, P. A., Spectroscopic Characterization of a Series of Platinum Acetylide Complexes Having a Localized Triplet Exciton. *J. Phys. Chem. A* **2006,** *110*, 4369-4375.
16. Rogers, J. E.; Slagle, J. E.; Krein, D. M.; Burke, A. R.; Hall, B. C.; Fratini, A.; McLean, D. G.; Fleitz, P. A.; Cooper, T. M.; Drobizhev, M., Platinum Acetylide Two-Photon Chromophores. *Inorg. Chem.* **2007,** *46*, 6483-6494.
17. Köhler, A.; Wittmann, H.; Friend, R. H.; Khan, M. S.; Lewis, J., Enhanced Photocurrent Response in Photocells Made with Platinum-Poly-yne/C60 Blends by Photoinduced Electron Transfer. *Synth. Met.* **1996,** *77*, 147-150.
18. Wong, W. Y.; Chan, S. M.; Choi, K. H.; Cheah, K. W.; Chan, W. K., Synthesis, Optical and Photoconducting Properties of Platinum Poly-yne Polymers Functionalized with Electron-Donating and Electron-Withdrawing Bithiazole Units. *Macromol. Rapid Commun.* **2000,** *21*, 453-457.
19. Zhao, X.; Cardolaccia, T.; Farley, R. T.; Abboud, K. A.; Schanze, K. S., A Platinum Acetylide Polymer with Sterically Demanding Substituents: Effect of Aggregation on the Triplet Excited State. *Inorg. Chem.* **2005,** *44*, 2619-2627.
20. Gray, T. G.; Liska, T.; Swetz, A.; Lai, P.-N.; Zeller, M.; Teets, T. S., Room-Temperature Phosphorescent Platinum (II) Alkynyls with Microsecond Lifetimes Bearing a Strong-Field Pincer Ligand. *Chem. Eur. J.* **2020**.
21. Na, H.; Wen, Z.; Judy, I.; Wu, C.; Teets, T. S., Mixed-Carbene Cyclometalated Iridium Complexes with Saturated Blue Luminescence. *Chem. Sci.* **2019,** *10*, 6254-6260.
22. Chi, Y.; Chou, P.-T., Transition-Metal Phosphors with Cyclometalating Ligands: Fundamentals and Applications. *Chem. Soc. Rev.* **2010,** *39*, 638-655.

23. Hopkinson, M. N.; Richter, C.; Schedler, M.; Glorius, F., An Overview of N-Heterocyclic Carbenes. *Nature* **2014,** *510*, 485-496.

24. Lee, J.; Chen, H.-F.; Batagoda, T.; Coburn, C.; Djurovich, P. I.; Thompson, M. E.; Forrest, S. R., Deep Blue Phosphorescent Organic Light-Emitting Diodes with Very High Brightness and Efficiency. *Nat. Materials* **2016,** *15*, 92-98.

25. Sajoto, T.; Djurovich, P. I.; Tamayo, A.; Yousufuddin, M.; Bau, R.; Thompson, M. E.; Holmes, R. J.; Forrest, S. R., Blue and near-Uv Phosphorescence from Iridium Complexes with Cyclometalated Pyrazolyl or N-Heterocyclic Carbene Ligands. *Inorg. Chem.* **2005,** *44*, 7992-8003.

26. Adamovich, V.; Boudreault, P.-L. T.; Esteruelas, M. A.; Gómez-Bautista, D.; López, A. M.; Oñate, E.; Tsai, J.-Y., Preparation Via a Nhc Dimer Complex, Photophysical Properties, and Device Performance of Heteroleptic Bis (Tridentate) Iridium (III) Emitters. *Organometallics* **2019,** *38*, 2738-2747.

27. Chen, Z.; Suramitr, S.; Zhu, N.; Ho, C.-L.; Hannongbua, S.; Chen, S.; Wong, W.-Y., Tetrafluorinated Phenylpyridine Based Heteroleptic Iridium (III) Complexes for Efficient Sky Blue Phosphorescent Organic Light-Emitting Diodes. *J. Mater. Chem. C* **2020,** *8*, 2551-2557.

28. Zhang, Y.; Blacque, O.; Venkatesan, K., Highly Efficient Deep-Blue Emitters Based on Cis and Trans N-Heterocyclic Carbene PtII Acetylide Complexes: Synthesis, Photophysical Properties, and Mechanistic Studies. *Chem. Eur. J.* **2013,** *19*, 15689-15701.

29. Bullock, J. D.; Salehi, A.; Zeman IV, C. J.; Abboud, K. A.; So, F.; Schanze, K. S., In Search of Deeper Blues: Trans-N-Heterocyclic Carbene Platinum Phenylacetylide as a Dopant for Phosphorescent OLEDs. *ACS Appl. Mater. Interfaces* **2017,** *9*, 41111-41114.

30. Bullock, J. D.; Valandro, S. R.; Sulicz, A. N.; Zeman IV, C. J.; Abboud, K. A.; Schanze, K. S., Blue Phosphorescent Trans-N-Heterocyclic Carbene Platinum Acetylides: Dependence on Energy Gap and Conformation. *J. Phys. Chem. A* **2019,** *123*, 9069-9078.
31. He, R.; Xu, Z.; Valandro, S.; Arman, H. D.; Xue, J.; Schanze, K. S., High-Purity and Saturated Deep-Blue Luminescence from Trans-Nhc Platinum (II) Butadiyne Complexes: Properties and Organic Light Emitting Diode Application. *ACS Appl. Mater. Interfaces* **2021,** *13*, 5327-5337.
32. Valandro, S. R.; He, R.; Bullock, J. D.; Arman, H.; Schanze, K. S., Ultrafast Excited-State Dynamics in Trans-(N-Heterocyclic Carbene) Platinum (II) Acetylide Complexes. *Inorg. Chem.* **2021,** *60*, 10065–10074.
33. Bullock, J. D.; Xu, Z.; Valandro, S.; Younus, M.; Xue, J.; Schanze, K. S., Trans-N-(Heterocyclic Carbene) Platinum (Ii) Acetylide Chromophores as Phosphors for OLED Applications. *ACS Appl. Electron. Mater.* **2020,** *2*, 1026-1034.
34. Pearson, D. L.; Schumm, J. S.; Tour, J. M., Iterative Divergent/Convergent Approach to Conjugated Oligomers by a Doubling of Molecular Length at Each Iteration. A Rapid Route to Potential Molecular Wires. *Macromolecules* **1994,** *27*, 2348-2350.
35. Hinderer, F.; May, R.; Jester, S.-S.; Höger, S., Monodisperse Oligo (P-Phenylene–Butadiynylene)s: GPC Conversion Factors and Self-Assembled Monolayers. *Macromolecules* **2016,** *49*, 1816-1821.
36. Hsu, H.-Y.; Vella, J. H.; Myers, J. D.; Xue, J.; Schanze, K. S., Triplet Exciton Diffusion in Platinum Polyyne Films. *J. Phys. Chem. C* **2014,** *118*, 24282-24289.

37. Rogers, J. E.; Cooper, T. M.; Fleitz, P. A.; Glass, D. J.; McLean, D. G., Photophysical Characterization of a Series of Platinum (II)-Containing Phenyl− Ethynyl Oligomers. *J. Phys. Chem. A* **2002,** *106*, 10108-10115.

38. Winkel, R. W.; Dubinina, G. G.; Abboud, K. A.; Schanze, K. S., Photophysical Properties of Trans-Platinum Acetylide Complexes Featuring N-Heterocyclic Carbene Ligands. *Dalton Transactions* **2014,** *43*, 17712-17720.

39. Schanze, K. S.; Silverman, E. E.; Zhao, X., Intrachain Triplet Energy Transfer in Platinum−Acetylide Copolymers. *J. Phys. Chem. B* **2005,** *109*, 18451-18459.

40. Sheng, C.-X.; Singh, S.; Gambetta, A.; Drori, T.; Tong, M.; Tretiak, S.; Vardeny, Z., Ultrafast Intersystem-Crossing in Platinum Containing π-Conjugated Polymers with Tunable Spin-Orbit Coupling. *Sci. Rep.* **2013,** *3*, 1-7.

41. Minaev, B.; Baryshnikov, G.; Agren, H., Principles of Phosphorescent Organic Light Emitting Devices. *Phys. Chem. Chem. Phys.* **2014,** *16*, 1719-1758.

42. Su, S.-J.; Sasabe, H.; Takeda, T.; Kido, J., Pyridine-Containing Bipolar Host Materials for Highly Efficient Blue Phosphorescent OLEDs. *Chem. Mater.* **2008,** *20*, 1691-1693.

43. Chang, C. F.; Cheng, Y. M.; Chi, Y.; Chiu, Y. C.; Lin, C. C.; Lee, G. H.; Chou, P. T.; Chen, C. C.; Chang, C. H.; Wu, C. C., Highly Efficient Blue-Emitting Iridium (III) Carbene Complexes and Phosphorescent OLEDs. *Angew. Chem. Int. Ed. Engl.* **2008,** *47*, 4542-4545.

44. Yang, C. H.; Cheng, Y. M.; Chi, Y.; Hsu, C. J.; Fang, F. C.; Wong, K. T.; Chou, P. T.; Chang, C. H.; Tsai, M. H.; Wu, C. C., Blue-Emitting Heteroleptic Iridium (III) Complexes Suitable for High-Efficiency Phosphorescent OLEDs. *Angew. Chem.* **2007,** *119*, 2470-2473.

45. Che, C. M.; Kwok, C. C.; Lai, S. W.; Rausch, A. F.; Finkenzeller, W. J.; Zhu, N.; Yersin, H., Photophysical Properties and Oled Applications of Phosphorescent Platinum (II) Schiff Base Complexes. *Chem. Eur. J.* **2010,** *16*, 233-247.

46. Wilson, J. S.; Dhoot, A.; Seeley, A.; Khan, M. S.; Köhler, A.; Friend, R. H., Spin-Dependent Exciton Formation in π-Conjugated Compounds. *Nature* **2001,** *413*, 828-831.

47. Wong, W.-Y.; Zhou, G.-J.; He, Z.; Cheung, K.-Y.; Ng, A. M.-C.; Djurišić, A. B.; Chan, W.-K., Organometallic Polymer Light-Emitting Diodes Derived from a Platinum(II) Polyyne Containing the Bithiazole Ring. *Macromol. Chem. Phys.* **2008,** *209*, 1319-1332.

48. Ho, C.-L.; Chui, C.-H.; Wong, W.-Y.; Aly, S. M.; Fortin, D.; Harvey, P. D.; Yao, B.; Xie, Z.; Wang, L., Efficient Electrophosphorescence from a Platinum Metallopolyyne Featuring a 2,7-Carbazole Chromophore. *Macromol. Chem. Phys.* **2009,** *210*, 1786-1798.

49. Giovanella, U.; Botta, C.; Papagni, A.; Tubino, R.; Miozzo, L., Electroluminescence from Two Fluorinated Organic Emitters Embedded in Polyvinylcarbazole. *App. Phys. Lett.* **2005,** *87*, 171910.

50. Germino, J. C.; de Freitas, J. N.; Domingues, R. A.; Quites, F. J.; Faleiros, M. M.; Atvars, T. D. Z., Organic Light-Emitting Diodes Based on Pvk and Zn (II) Salicylidene Composites. *Synth. Met.* **2018,** *241*, 7-16.

51. Jiang, X.; Register, R. A.; Killeen, K. A.; Thompson, M. E.; Pschenitzka, F.; Hebner, T. R.; Sturm, J. C., Effect of Carbazole–Oxadiazole Excited-State Complexes on the Efficiency of Dye-Doped Light-Emitting Diodes. *J. App. Phys.* **2002,** *91*, 6717-6724.

52. Glusac, K.; Köse, M. E.; Jiang, H.; Schanze, K. S., Triplet Excited State in Platinum−Acetylide Oligomers: Triplet Localization and Effects of Conformation. *J. Phys. Chem. B* **2007,** *111*, 929-940.

53. Goudreault, T.; He, Z.; Guo, Y.; Ho, C.-L.; Zhan, H.; Wang, Q.; Ho, K. Y.-F.; Wong, K.-L.; Fortin, D.; Yao, B.; Xie, Z.; Wang, L.; Kwok, W.-M.; Harvey, P. D.; Wong, W.-Y., Synthesis, Light-Emitting, and Two-Photon Absorption Properties of Platinum-Containing Poly(Arylene-Ethynylene)S Linked by 1,3,4-Oxadiazole Units. *Macromolecules* **2010,** *43*, 7936-7949.

Table of Contents Graphic